

Abundances and ADFs in PNe with [WC] central stars

J. García-Rojas¹ †, M. Peña², C. Morisset^{1,2} and M. T. Ruiz³

¹IAC, E-38200, La Laguna, Tenerife, Spain. email: jogarcia@iac.es

²IA-UNAM. Apdo Postal 70264, Mex. D. F., 04510 Mexico. email: miriam@astroscu.unam.mx, chris.morisset@gmail.com

³DAS. U. Chile. Casilla 36D, Santiago, Chile. email: mtruiz@das.uchile.cl

Abstract. We present preliminary results obtained from the analysis of very deep echelle spectra of a dozen planetary nebulae with [WC] or weak emission lines (wels) central stars. The computed abundance discrepancy factors (ADFs) are moderate, with values lower than 4. In principle, no evidence of the H-poor metal enriched inclusions proposed by Liu et al. (2000) have been found. However, a detailed analysis of the data is in progress.

Keywords. stars: AGB and post-AGB, ISM: abundances, ISM: planetary nebulae: general

1. Introduction and Observations

PNe around [WR] central stars constitute a particular photoionized nebula class, representing about 10-15% of the PNe with known progenitor. In principle, these PNe seem suitable for analyzing the abundance discrepancy found when computing abundances from faint recombination lines (RLs) or from collisional excited lines (CELs). Liu et al. (2000) proposed the presence of H-deficient knots embedded in the hot plasma as responsible of large ADFs (i.e. RLs/CELs abundance ratios). These knots could be plausible around H-poor WR stars. High spectral resolution spectra were obtained with MIKE echelle spectrograph in the 6.5m Clay Magellan Telescope at Las Campanas Observatory (Chile) The spectral resolution varied from $\sim 10.8 \text{ km s}^{-1}$ in the blue to $\sim 12.8 \text{ km s}^{-1}$ in the red. Data were reduced and flux calibrated.

2. Plasma Diagnostics and Chemical abundances

We have obtained physical conditions, T_e and n_e , from several diagnostic line ratios by using state-of-the-art atomic data and a preliminary version of the package PyNEB of IRAF (see Luridiana et al. 2011). We have constructed T_e vs. n_e diagnostic plots for each object. In general, we have found that $n_e([\text{Ar IV}]) > n_e([\text{Cl III}]) > n_e([\text{S II}]) > n_e([\text{OII}])$. Low-ionization electron temperature, $T_e([\text{N II}])$, was corrected from the effect of recombination contribution to the auroral [N II] $\lambda 5755$ line. In Figure 1a. we show the behavior of $T_e([\text{O III}])/T_e([\text{N II}])$ ratio with the O^{++}/O^+ . For comparison we include data from Peña et al. (2001) –WR PNe, red– and from Gorny et al. (2009) –Non WR PNe, blue–. There is a tendency to lower temperature ratio with the increasing O^{++}/O^+ . This tendency could not be explained by photoionization models and should be investigated further.

Ionic abundances of several heavy metal ions were computed from CELs. We used $T_e([\text{N II}])$, $T_e([\text{O III}])$ and $T_e([\text{Ar IV}])$, when available for the low, intermediate and

† Based on data collected at Las Campanas Observatory, Chile.

high ionization zones, respectively. Total abundances were obtained using the set of ICFs proposed by Kingsburgh & Barlow (1994). Since most of the ICFs depend on the ionization degree (O^+/O) which in turn depends strongly on the adopted n_e , we have explored the behavior of Ne/H ratio *vs.* O/H ratio in Figure 1b. by using an averaged n_e (open triangles) or by assuming $n_e([Cl\ III])$ as characteristic of the whole nebula (filled triangles). The dispersion in the relationship between Ne/H (which is an α element) and O/H is clearly lower when adopting $n_e([Cl\ III])$, and this effect is especially important in the high density objects, where $[O\ II]$ and $[S\ II]$ n_e diagnostics are saturated. Two objects, whatever density is used, have very low neon abundance. A more detailed abundance study is in progress.

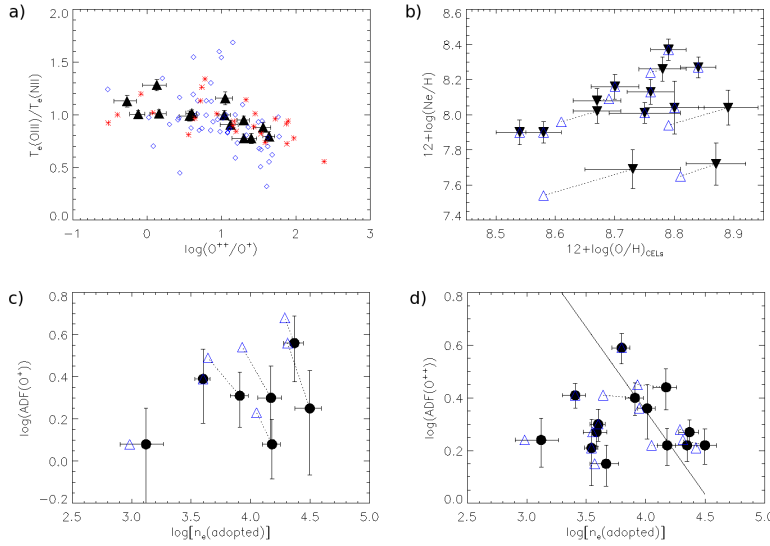


Figure 1. a) Temperature ratio *vs.* ionization degree. b) Ne/H *vs.* O/H. c) ADF(O^+) *vs.* n_e d) ADF(O^{++}) *vs.* n_e . The relationship found by Robertson-Tessi & Garnett (2005) is shown.

3. Abundance Discrepancies

The ADF was computed for O^+/H^+ and O^{++}/H^+ ratios. In Figure 1c. and 1d. we show the behavior of both ADFs with the adopted n_e , respectively. The influence of the adopted density (averaged, open symbols) or $n_e([Cl\ III])$ (filled symbols) is also showed. It is clear the influence of the adopted density on the computed ADF(O^+). This effect is very small in the derived ADFs(O^{++}). From that Figure we can also see that ADFs are always moderate for both ions (O^+ and O^{++}) in these objects. No direct evidence for the presence of cold and high density clumps has been found.

References

- Gorny, S.K., Stasińska, G., Escudero, A.V., & Costa, R.D.D. 2009, *AA*, 427, 231
- Kingsburgh, R.L., & Barlow, M.J. 1994, *MNRAS*, 271, 257
- Liu, X.-W., Storey, P.J., Barlow, M.J., et al. 2000, *MNRAS*, 312, 585
- Luridiana, V., Shaw, D., & Morisset, C. 2011, *This proceedings*
- Peña, M., Stasińska, G., & Medina, S. 2001, *AA*, 367, 983
- Robertson-Tessi, M., & Garnett, D.R. 2005, *ApJS*, 157, 371